Original Research Paper   **Open Access**

Effects of a Novel Soil Remediation Agent on Cadmium Contaminated Soil

Chuang Ma*†, Bin Hu*, Fu-Yong Liu*, Chang-Chang Jia*, Ming-Bao Wei* and Hong-Zhong Zhang**

*Zhengzhou University of Light Industry, Zhengzhou 450001, PR China

**Collaborative Innovation Center of Environmental Pollution Control and Ecological Restoration, Henan Province, Zhengzhou 450001, PR China

†Corresponding author: Chuang Ma

ABSTRACT

A novel type of NH_2-functionalized carbon-coated Fe_3O_4 core-shell nanoparticles (Fe_3O_4@C-NH_2) soil remediation agent was prepared. The effects of the Fe_3O_4@C-NH_2 application rate, pH, water content, soil conductivity, soil organic matter (SOM) and solidification time on the solidification efficiency of cadmium (Cd) in Cd-contaminated soils were investigated. The results showed that the structure of Fe_3O_4@C-NH_2 had a hollow core-shell, the carbon shell was well dispersed, the -NH_2 bonding was obvious and the adsorption of Fe_3O_4@C-NH_2 to Cd^{2+} in water quickly reached equilibrium within 20 min, with a saturated adsorption capacity of 78.83 mg.g^{-1}. The Fe_3O_4@C-NH_2 application rate and soil organic matter (SOM) had a great influence on solidification efficiency. SOM mainly affected the transition from weak acidity to reducible and oxidizable state, while solidification time affected the transition from oxidizable state to residual state. The optimal conditions for Fe_3O_4@C-NH_2 solidification of Cd are: application rate of 3%-4% (3.3%), pH of 6-10 (7.33), moisture content of 40%-60% (50%), conductivity of 90-400 µS.cm^{-1} (142.6 µS.cm^{-1}), SOM of 45.00-65.00 g.kg^{-1} (63.04 g.kg^{-1}) and solidification time of no less than 10 days. Under the optimal conditions, the solidification efficiency of Fe_3O_4@C-NH_2 for Cd was 42.95±1.89%, which significantly reduced the leaching and migration of Cd and achieved the goal of remediation.

INTRODUCTION

There is serious soil pollution in some areas of China, which is responsible for deteriorating soil quality. Among soil pollutants, heavy metals such as cadmium, lead, zinc and nickel account for 82.8% of all sites that are above the standard guideline values, with Cd polluted sites accounting for up to 7%. It is, therefore, urgent to implement the remediation of heavy metal contaminated soils. Traditional remediation agents such as phosphates, lime and organic reagents are commonly used in the process of stabilization remediation of heavy metal contaminated soil. However, they all have certain limitations: 1. Because of the lack of specific functional groups, traditional restoration agents do not demonstrate strong adsorption, chelation and coordination of heavy metals, so their specificity is poor; 2. High application rates are required, mostly in the range of 10%-20% and the labour and production costs are high; 3. The remediation time is long, up to 3-4 months, which can seriously affect the remediation progress; 4. Traditional adsorbents can affect soil structure and properties, leading to the risk of leaching and groundwater pollution (Xu et al. 2017). Therefore, it is necessary to develop new environmental-friendly soil stabilizers to overcome the above-mentioned shortcomings.

Magnetic nanomaterials are widely used in the environment because of several advantages like large adsorption capacity, fast adsorption rate and recyclability (Zhang et al. 2013). In this paper, a novel type of Fe_3O_4@C-NH_2 remediation agent for Cd-contaminated soil was prepared. The effects of Fe_3O_4@C-NH_2 on the distribution of chemical forms of Cd in soil were analysed by the European Community Standard of Reference (BCR) extraction method. The results will provide a theoretical basis for the remediation of Cd-contaminated soil with functional magnetic nanomaterials.

MATERIALS AND METHODS

Cd-contaminated soil: Cd contaminated soils were collected from 0-25 cm topsoil of Cd-contaminated farmland near a lead-zinc smelter (east longitude 112°33'21'', north latitude 35°8'26'') in Henan Province, China. The soils were naturally air-dried, ground in an agate mortar, sieved through 100-mesh sieve and packed in bags. The soil physical and chemical properties are given in Table 1.

Preparation of Fe_3O_4@C-NH_2: As shown in Fig. 1, monodisperse silicon dioxide (SiO_2) template microspheres with an average diameter of 400 nm were prepared by a modified Stober method and stored after freeze-drying as

Table 1: Soil physical and chemical properties and morphological distribution.

pH	EC µS.cm⁻¹	Organic matter g.kg⁻¹	Total Cd mg.kg⁻¹	Weak acid state mg.kg⁻¹	Reducible state mg.kg⁻¹	Oxidizable state mg.kg⁻¹	Residual state mg.kg⁻¹
7.33	142.60	20.13	5.61	3.39(60.59%)	1.71(30.41%)	0.31(5.53%)	0.20(3.57%)

Notes: EC is electrical conductivity

follows: The analytical balance was used to weigh 50.6 mg of SiO_2 at 400 nm in 60 mL acetone for 10 min, then 0.2012 g of ferrocene in acetone was added and incubated for 30 min. Hydrogen peroxide was added drop by drop at the same time with magnetic stirring. After 2 h of magnetic stirring, the preparation was placed in a 50 mL polytetrafluoroethylene (PTFE) autoclave at 210°C for 48 h. After centrifugal washing, it was freeze-dried. $SiO_2@Fe_3O_4@C$ magnetic nanomaterials were prepared as previously described (Cheng et al. 2013). $SiO_2@Fe_3O_4@C$ was etched to form hollow microspheres of $Fe_3O_4@C$. A total of 80 mg of the freeze-dried gray-black powder ($Fe_3O_4@C$) was placed in a beaker with 48 mL deionized water and ultrasonically dispersed for 2 min; 24 mL ammonia water was added and shaken, then the suspension was quickly poured into a 100 mL PTFE autoclave and hydrothermally reacted at 160°C for 6 h. The materials were then cooled to room temperature and freeze-dried after centrifugal washing (Li et al. 2015). The above materials (200 mg) were dispersed in 40 mL acetone, 1 drop of ammonia water was added with mechanical stirring for 15 min, then the materials were heated to 60°C to undergo reflux condensation; 1 mL 3-aminopropyl triethoxysilane was then added with mechanical stirring for 12 h at 250 rpm. After centrifugal washing and freeze-drying, hollow $Fe_3O_4@C\text{-}NH_2$ magnetic nanomaterials were obtained.

Adsorption experiments in water: Cadmium nitrate was used to prepare a series of Cd^{2+} solutions with concentration of 0-24 mg.L⁻¹. The pH was adjusted with dilute hydrochloric acid and sodium hydroxide. The above Cd^{2+} solutions were then placed in 25 mL centrifuge tubes with 2 mg $Fe_3O_4@C\text{-}NH_2$. After mixing, the supernatant was shaken by a constant temperature oscillator (30°C). After magnetic sepa-

ration, the supernatant was removed. Finally, the concentration of Cd was determined by atomic absorption spectrometer (ZEEnit-700P, Analytik Jena AG, Jena, Germany).

Material characterization methods: The samples were characterized by X-ray diffraction (XRD) (D8 Advance, Bruker, Germany), and transmission electron microscopy (TEM)(JEM-2100, JEOL Ltd, Japan). The appearance and morphology of the material were characterized by JSM-6490LV (JEOL Ltd., Japan) scanning electron microscopy (SEM). The material was analysed by using Nicolet iS50 (Thermo Fisher Scientific Inc., US) Fourier Transform Infrared Spectrometer.

Experimental design: The experimental treatments were prepared to investigate the effect of remediation agent application rate, soil pH, water content, conductivity and organic matter content on soil remediation as follows:

(1) Remediation agent application rate: 0.6%, 1.3%, 2.0%, 2.6%, 3.3% and 4.0% (w/w) of remediation agent were added to contaminated soil. After 5 days of exposure, the chemical speciation of soil samples was analysed to determine the effect of remediation agent application rate on Cd speciation.

(2) Soil pH: To investigate the effect of pH on the efficacy of the remediation agent, HNO_3 and NaOH were used to regulate the pH of the tested soils. After aging, the measured pH values were 6.41, 6.92, 7.33, 7.96, 8.52 and 9.87. $Fe_3O_4@C\text{-}NH_2$ was added at 3.3% (w/w). After 5 days of exposure, 1.5 g of soil was taken for chemical speciation analysis to determine the effect of soil pH on speciation of Cd.

(3) Water content: 3.3% $Fe_3O_4@C\text{-}NH_2$ was added to contaminated soil and the water content was adjusted to

A:9ml NH₄OH+16.25mlC₂H₅OH +24.75ml H₂O
B:4.5mlC₈H₂₀O₄Si+45.5mlC₂H₅OH

50.6mg SiO₂+60mlCH₃COCH₃ 0.2102g Fe(C₅H₅)₂+2mlH₂O₂

80mg SiO₂ @Fe₃O₄@C +48mlH₂O +24mlNH₄OH

200mg Fe₃O₄@C+40mlCH₃COCH₃ +1drop NH₄OH 15min 60°C 1mlAPTES

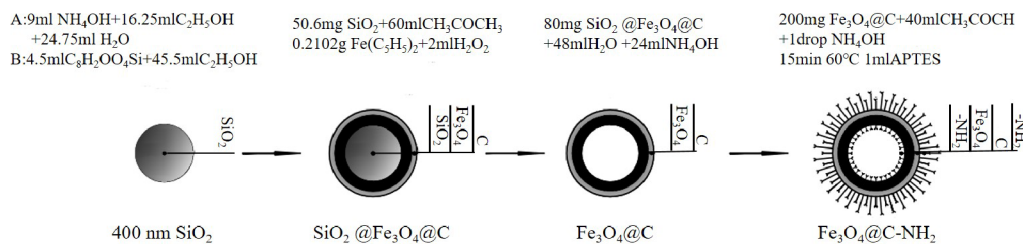400 nm SiO₂   SiO₂ @Fe₃O₄@C   Fe₃O₄@C   Fe₃O₄@C-NH₂

Fig. 1: Remediation agent preparation process.
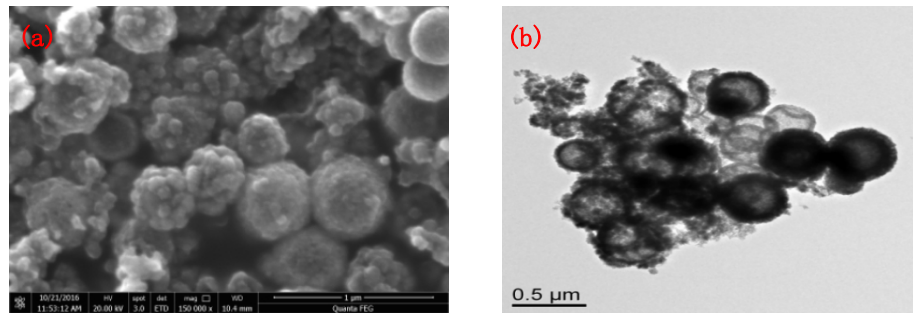
Fig. 2: Scanning electron microscopy (a) and transmission electron microscopy (b) of Fe_3O_4@C-NH_2.

20%, 30%, 40%, 50%, 60% and 70%; the pH for all treatments was 7.33. After 5 days of exposure, 1.5 g of soil was taken for chemical speciation analysis to determine the effect of soil water content on speciation of heavy metals.

(4) Conductivity: The effects of Fe_3O_4@C-NH_2 on the chemical morphology of Cd under different conductivity conditions were studied when the dosage of Fe_3O_4@C-NH_2 was 3.3%, the pH was 7.33 and the moisture content was 50%. The effect of remediation time on the Cd speciation was studied with the conductivity adjusted to 96.5, 142.6, 175.4, 253.1, 316.2, 358.1 and 358.1 $\mu S.cm^{-1}$.

(5) To explore the effect of soil organic matter (SOM) on Cd speciation, it was necessary to find out whether the remediation agent or SOM was more important in the solidification process. With the SOM content of the original soil as the boundary, treatments 1, 2 and 3 were prepared. Treatment 1 was designed to study the effects of high SOM content alone (20.13, 32.33, 45.26, 51.72, 63.04 and 79.20 $g.kg^{-1}$); treatment 2 was designed to study the combined effects of high SOM content (20.13 $g.kg^{-1}$, 32.33 $g.kg^{-1}$, 45.26 $g.kg^{-1}$, 51.72 $g.kg^{-1}$, 63.04 $g.kg^{-1}$, 79.20 $g.kg^{-1}$) and remediation agent (3.3% Fe_3O_4@C-NH_2); treatment 3 used a burning method to reduce the SOM concentration in soil (0.24, 5.78, 10.11, 15.62 and 20.13 $g.kg^{-1}$).

Chemical analysis: The pH was determined by potentiometry (Jayasinghe 2009). The moisture content was determined by drying method (Liu 2017). The conductivity was determined by the 5:1 extraction method (Jayasinghe 2009). Organic matter was determined by the potassium dichromate-concentrated sulphuric acid external heating method. The Cd content in water and soil was determined by atomic absorption spectrometer (ZEEnit-700P).

The modified BCR method was used for sequential extraction of heavy metals from soil. The stability of the weak acid and reducible fractions was poor and could be taken up by crops or leached. Therefore, the solidification efficiency of the remediation agent was evaluated by the percentage of weak acidity, reducible fraction or oxidizable state of heavy metals, and by the increase in the residual state relative to that of the total amount of Cd.

The formula for calculating the solidification rate is as follows:

$$N = \frac{a+b}{F} \qquad ...(1)$$

Where, a is the reducible fraction, b is the weak acid fraction, F is the total Cd and N is the solidification rate.

RESULTS AND DISCUSSION

Characterization of Materials

Characterization and analysis of the remediation agent by SEM and TEM: The morphology of Fe_3O_4@C-NH_2 was analysed by SEM and TEM. It could be clearly seen that the inner colour of the material was light and the layers were obvious. Hollow microspheres were formed with uniform particle size and good dispersion. They had a hollow core-shell structure (Fig. 2). The particle size distribution showed that the particle size of hollow microspheres was about 400 nm (Fig. 2a). The order from inside to outside was Fe_3O_4 hollow microspheres, carbon shells and functional groups. The inner layer was hollow Fe_3O_4; the hollow Fe_3O_4 nanospheres were non-toxic and had good biocompatibility, which meant that they would not destroy the soil structure and properties and had no effect on groundwater during their use. Although Fe_3O_4 nanoparticles are highly competent as conductive fillers, two limitations have been identified in their practical applications: (1) Fe_3O_4 nanoparticles readily aggregate because of their large specific surface area and high surface free energy, making nanoscale dispersion of Fe_3O_4 nanoparticles in a polymer matrix extremely challenging; (2) Fe_3O_4 nanoparticles can
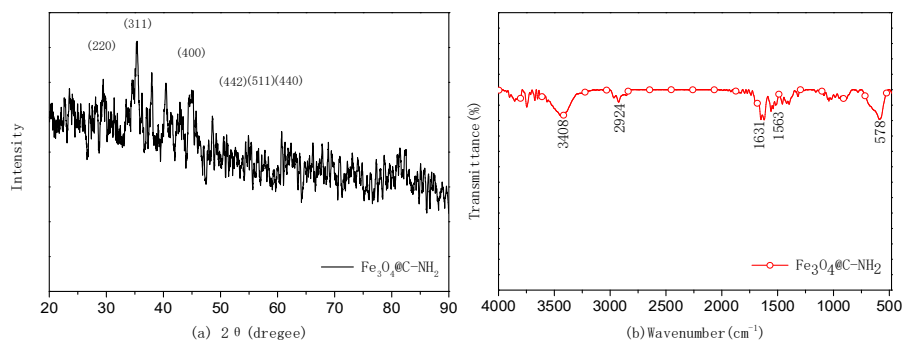
Fig. 3: X-ray diffraction (a), and Fourier transform infrared spectroscopy (b) of Fe_3O_4@C-NH_2
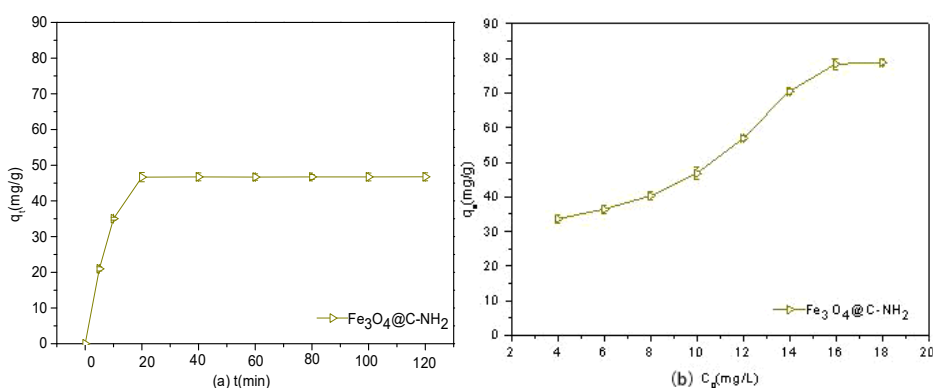

Fig. 4: (a) Effect of adsorption time on the adsorption quantities and (b) effect of initial concentration on the adsorption quantities.

be easily oxidized in the absence of a protective shell. To overcome these barriers, the middle layer was carbon shell, which could protect Fe_3O_4 from oxidation and prevent the reunion of Fe_3O_4, and maintain excellent stability under acid-base, high temperature and high pressure conditions. The stability ensured a wide range of pH in the soil.

XRD and infrared spectrum characterization analysis:
The crystal structure of Fe_3O_4@C-NH_2 was characterized by XRD (Fig. 3a). The characteristic 2θ peaks of aminated Fe_3O_4@C magnetic nanomaterials were found at 30.1°, 35.5°, 43.2°, 53.4°, 57.1° and 62.6°. The diffraction fronts belonged to (220), (311), (400), (442), (511), (440) crystal shapes and their corresponding structures. Both of them were basically consistent with the standard XRD spectra of Fe_3O_4, but the width of the diffraction peaks was different, which was related to the change in particle size. The XRD characteristic peaks of aminated Fe_3O_4@C-NH_2 were relatively weak, indicating that the presence of functional groups weakened the intensity of the characteristic peaks, and indicated that some substance adhered to the material.

The functional groups and chemical composition of Fe_3O_4@C-NH_2 were characterized by Fourier transform

infrared spectroscopy (Fig. 3b). The absorption peak at 578 cm^{-1} was the characteristic absorption peak of Fe_3O_4. The absorption peak at 1631 cm^{-1} corresponded to the stretching vibration of C=O, 2924 cm^{-1} corresponded to the stretching vibration peak of C-H, 1563 cm^{-1} corresponded to the bending vibration absorption peak of N-H and 3408 cm^{-1} corresponded to the stretching vibration absorption peak of N-H. These results showed that the -NH_2 group was attached to the Fe_3O_4@C surface (Yang et al. 2005).

Combined with the functional groups observed on the outermost surface (Fig. 2a and b), the Fe_3O_4@C hollow microspheres had a large number of functional groups of -NH_2 and -OH. The hollow core-shell structure facilitated the attachment of a layer of functional groups to the surface of the material, and also facilitated the attachment of a layer of functional groups to the interior of the material. These functional groups not only enhanced the specific adsorption of Cd, but also enhanced the solid adsorption. These functional groups were the active centres of Fe_3O_4@C adsorption.

Adsorption characteristics of materials in water: The adsorption equilibrium of the material was established after

20 min of oscillation, and the adsorption rate was fast (Fig. 4a); the saturated adsorption capacity of Fe_3O_4@C-NH_2 was 78.83 mg.L^{-1} (Fig. 4b).

The experimental data of Fe_3O_4@C-NH_2 adsorption of Cd^{2+} were fitted to a quasi-second-order kinetic equation. The model equation was as follows:

$$\frac{t}{q_t} = \frac{1}{K_{ad}q_e^2} + \frac{1}{q_e}t \qquad ...(2)$$

Where, q_t is the adsorption capacity of heavy metal ions absorbed by adsorbents at time t (min), mg.g^{-1}, q_e is the adsorption capacity of heavy metal ions absorbed by adsorbents at adsorption equilibrium, mg.g^{-1}, and K_{ad} is the rate constant of quasi-second-order adsorption kinetics equation, g mg^{-1}min^{-1}. The curve of the Fe_3O_4@C-NH_2 simulated quasi-second-order dynamic equation is shown in Fig. 5a, where, t/q_t plots t as a straight line. The values for q_e, K_{ad} and R^2 are given in Table 2.

The correlation coefficient (R^2) was approximately equal to 1 (Table 2), which showed a good correlation. Fig. 4a also showed that the fitting curve and data points were coincident, so the quasi-second-order kinetic equation adequately described the Cd^{2+} adsorption process on magnetic materials at different times. This indicated that the rate-limiting step of adsorption was controlled by the chemical adsorption between adsorbent and adsorbate, and was not affected by the mass transfer in solution (Wang et al. 2017).

Table 2: Quasi-second-order kinetic equation fitting data.

Category	Equation	R^2	Kad	qe
Fe_3O_4@C-NH_2	y=0.04902+0.02085x	0.9978	0.00886	47.96

Solidification of Cd in Contaminated Soil by Remediation Agent

Effect of soil remediation agent application rate on solidification efficiency: The Fe_3O_4@C-NH_2 remediation agent was added to Cd-contaminated soil at 0.6%, 1.3%, 2.0%, 2.6%, 3.3% and 4.0% (w/w). The solidification efficiency of Cd increased rapidly at first and then remained basically unchanged. The remediation efficiency was 1.91±0.25%, 2.75±0.49%, 4.31±0.73%, 8.32±1.30%, 15.01±1.11% and 15.59±1.26%, respectively (Fig. 5a). The content of weak acidic and reducible Cd gradually decreased, while the content of oxidizable Cd remained basically unchanged, and the content of residual Cd gradually increased. However, when the application rate exceeded 3.3%, the rate of change tended to decrease. Although the weak acidity decreased

and the residual state increased, the change was not significant. This might be because of the saturation of the adsorption sites on the surface of the remediation agent by heavy metal ions. Although the dosage continued to increase, the effect remained unchanged.

Effects of soil pH on solidification efficiency: The pH values of Cd-contaminated soils were 6.41, 6.92, 7.33, 7.96, 8.52 and 9.87; 3.3% (w/w) Fe_3O_4@C-NH_2 was added to Cd-contaminated soils. After 10 days of exposure, the solidification efficiency of Cd gradually increased, but the trend was slow and basically remained unchanged. The remediation efficiency of Cd was 10.61±0.42%, 13.61±1.14%, 14.79±0.68%, 15.86±0.90%, 16.64±1.08% and 16.18±1.11%, respectively (Fig. 6b). With the increase in pH, the content of weak acidic and reducible Cd gradually decreased, while the content of oxidizable Cd remained basically unchanged, and the content of residual Cd gradually increased. With the change in starting pH in this experiment from 6.41 to 9.87, the remediation efficiency did not change substantially, that is, the remediation agent had a wide range of application and strong acid and alkali resistance.

Effects of soil water content on solidification efficiency: In the process of soil stabilization remediation, water is an important medium to promote the combination of remediation agents and heavy metals. 3.3% Fe_3O_4@C-NH_2 was added to Cd contaminated soil, and the water content was adjusted to 20%, 30%, 40%, 50%, 60% and 70%. After 10 days of exposure, the solidification efficiency of Cd gradually increased and then decreased. The solidification efficiency of Cd was 2.91±0.48%, 8.69±0.64%, 12.75±1.74%, 14.71±0.95%, 14.54±1.43% and 14.29±1.37%, respectively (Fig. 6c). With the increase in water content, the content of weak acidic Cd first decreased and then increased, the content of reducible Cd first decreased and then increased, the content of oxidizable Cd first increased and then decreased, and the content of residual Cd first increased and then decreased. When the water content was >50%, the rate of change tended to decrease, resulting in an increase in the weak acid and residual state. These results established that a suitable moisture content range was 40%-60% and the optimum moisture content was 50%.

Effect of soil conductivity on solidification efficiency: Soil is composed of a series of complex components. 3.3% Fe_3O_4@C-NH_2 was added to Cd contaminated soil, and the electrical conductivity was adjusted to 96.5, 142.6, 175.4, 253.1, 316.2 and 358.1 μS.cm^{-1}. The moisture content was 50% after 10 days of exposure. The solidification efficiency of Cd gradually increased and then remained basically unchanged. The solidification efficiency of Cd was
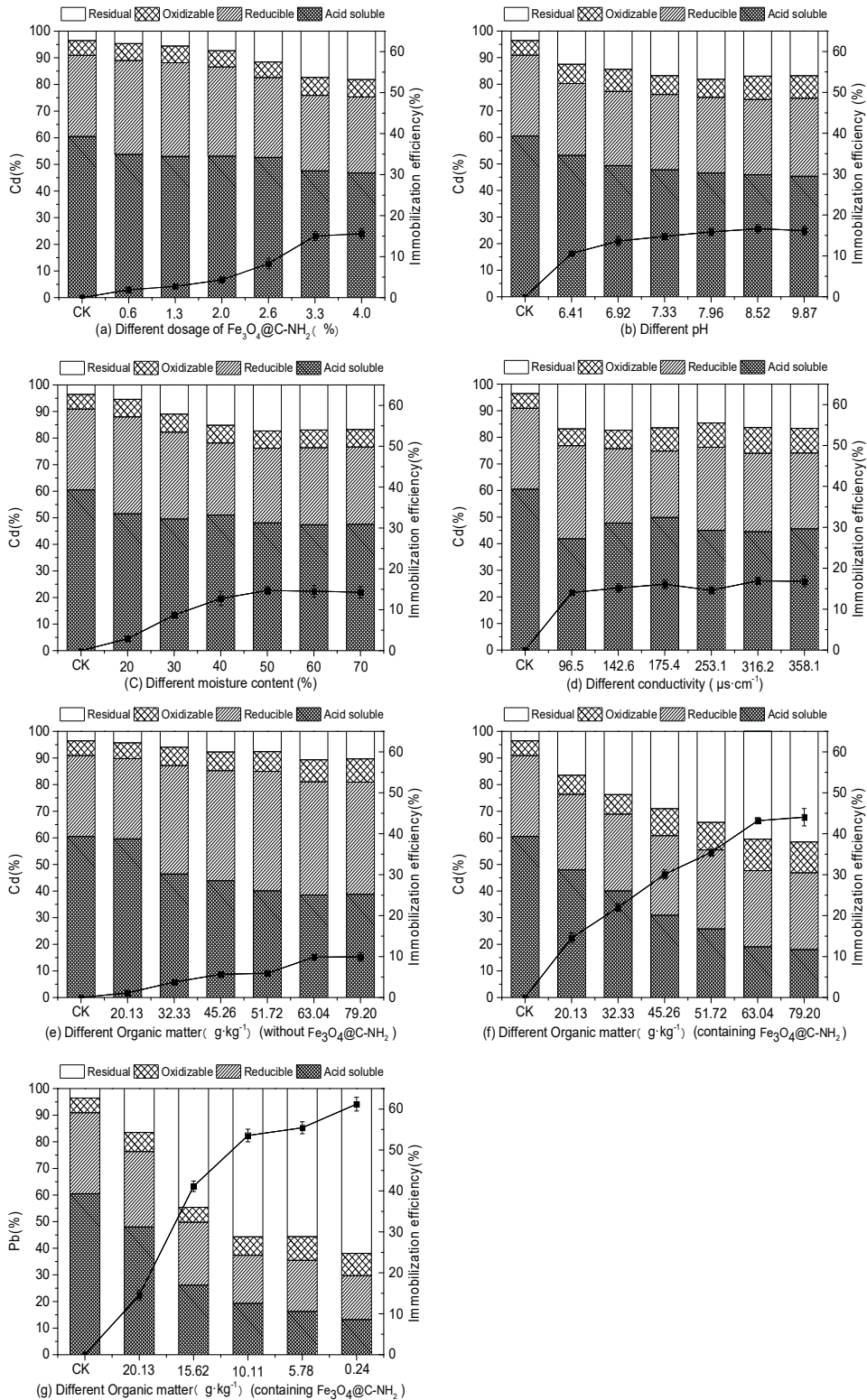
Fig. 5: Effect of Fe₃O₄@C-NH₂ dosage (a), pH (b), moisture content (c), conductivity (d), and soil organic matter (e, f, g) on the cadmium (Cd) speciation and immobilization efficiency in Cd-contaminated soil
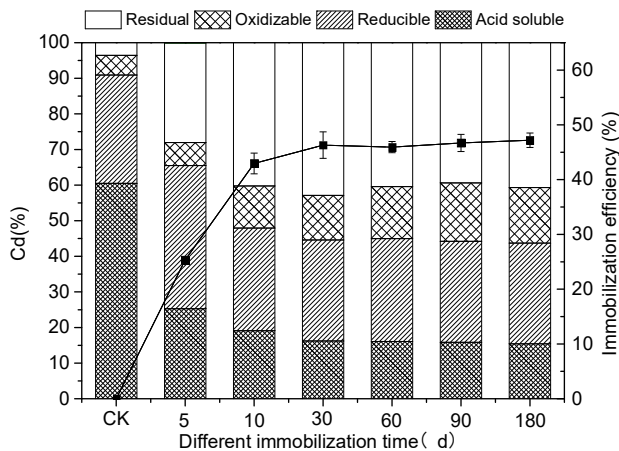
Fig. 6: Effect of immobilization time on the speciation and immobilization efficiency of Cd.

$14.04\pm0.63\%$, $15.18\pm1.05\%$, $16.07\pm1.08\%$, $14.61\pm0.85\%$, $16.92\pm0.89\%$ and $16.80\pm1.31\%$, respectively (Fig. 6d). With the increase in conductivity, the content of weak acidic Cd gradually increased, the content of reducible Cd gradually decreased, the content of oxidizable Cd gradually increased, and the content of residual Cd gradually increased. Higher conductivity increased the weak acidity of heavy metals in soil and increased the biological toxicity of heavy metals. However, when the conductivity was >142.6 $\mu S.cm^{-1}$, the rate of change in weak acidic Cd tended to ease and then slowly decreased. Although the weak acidity and residual state increased, the remediation efficiency did not change significantly. This indicated that the remediation agent was tolerant to a wide range of salinity, and the conductivity could be controlled between 90 and 400 $\mu S.cm^{-1}$.

Effects of SOM on solidification efficiency: With the increase in SOM in treatment 1, the solidification efficiency also increased. The solidification efficiency was $1.12\pm0.31\%$, $3.77\pm0.59\%$, $5.67\pm0.62\%$, $5.93\pm0.44\%$, $9.85\pm0.50\%$ and $9.94\pm1.05\%$ (Fig. 6e) for SOM contents of 20.13, 32.33, 45.26, 51.72, 63.04 and 79.20 g kg^{-1}, respectively. With the increase in SOM content, the contents of weak acidity and reducible state of Cd decreased, and the contents of oxidizable state and residual state of Cd increased. However, when the SOM content was >63.04 g.kg^{-1}, the rate of change tended to decrease. When considering the solidification efficiency and cost, the suitable range of SOM content was 45.00-65.00 g.kg^{-1}, and the optimum SOM content was 63.04 g.kg^{-1}. With the increase in SOM content, the solidification efficiency first decreased, then increased, and finally remained unchanged. The remediation efficiency in treatment 2 was $14.55\pm1.24\%$, $22.02\pm0.95\%$, $30.09\pm1.10\%$, $35.44\pm0.93\%$, $43.19\pm0.74\%$ and $44.04\pm2.13\%$ for 20.13, 32.33, 45.26, 51.72, 63.04 and 79.20 g. kg^{-1}, respectively,

with 3.3% Fe$_3$O$_4$@C-NH$_2$ (Fig. 6f). The solidification efficiency of treatment 3 increased with the decrease in SOM content. The remediation efficiency was $14.55\pm1.24\%$, $41.13\pm1.28\%$, $53.54\pm1.55\%$, $55.43\pm1.47\%$ and $61.20\pm1.68\%$ (Fig. 6g).

When comparing treatments 1 and 2, the solidification efficiency of SOM for Cd was $9.85\pm0.50\%$ when high concentrations of SOM were used alone in treatment 1. The solidification efficiency of Fe$_3$O$_4$@C-NH$_2$ for Cd was $43.19\pm0.74\%$ when treated with Fe$_3$O$_4$@C-NH$_2$ and high concentrations of SOM in treatment 2 (for 20.13, 45.26, 63.04, 79.20 g.kg^{-1} SOM). It was concluded that the solidification efficiency of Cd by Fe$_3$O$_4$@C-NH$_2$ alone was $33.34\pm1.24\%$. Under the combined action of the remediation agent and high concentration of SOM, the remediation agent played a dominant role and the SOM played an auxiliary role. When the content of SOM was 0.24 g.kg^{-1} and the remediation agent was Fe$_3$O$_4$@C-NH$_2$, the content of weak acidic Cd reached the lowest level, and the solidification efficiency reached $61.20\pm1.68\%$ in only 10 days. The reason for this might be that when the burning method was used to reduce the SOM content, only minerals were left after heating decomposition of organic matter, which reduced the adsorption capacity of SOM to heavy metals and released heavy metals.

Therefore, considering the difficulty of engineering construction and technical feasibility, the SOM content could be increased (the optimum value of adjusted SOM content was 63.04 g.kg^{-1}) to obtain higher solidification efficiency.

Rehabilitation Effect and Stability Evaluation

Stability of the remediation effect: To verify the long-term stability of the remediation effect and ensure that it did not change with time, 3.3% Fe$_3$O$_4$@C-NH$_2$ was added to Cd-contaminated soil, with SOM adjusted to 63.04 g.kg^{-1} and water content of 50%. Samples were taken at 5, 10, 30, 60, 90 and 180 days. The remediation efficiency of Cd increased slowly at first and then remained basically unchanged. The remediation efficiency was $25.36\pm0.55\%$, $42.95\pm1.89\%$, $46.30\pm2.42\%$, $45.94\pm1.03\%$, $46.69\pm1.57\%$ and $47.19\pm1.32\%$, respectively (Fig. 6). The remediation efficiency at 10 days ($42.95\pm1.89\%$) was slightly lower than that of 30 days ($46.30\pm2.42\%$); however, when considering the solidification remediation efficiency and time, it is most appropriate to choose 10 days as the appropriate solidification time. At this time, the weak acid state, reducible state, oxidizable state and residual state of Cd changed from 60.50%, 30.41%, 5.53% and 3.57% to 19.11%, 28.84%, 11.81% and 40.24%, respectively.

Table 3: Leaching concentration of cadmium (Cd) before and after remediation.

	Cd(mg.kg^{-1})
Original soil	1.96
TCLP leaching after repairation	
Fe$_3$O$_4$@C-NH$_2$	0.40
Standard limit	0.50

Notes: The standard limit refers to GB5085.3-2007

Toxicity leaching test of toxicity characteristic leaching procedure (TCLP): Biotoxicity of heavy metals is not only related to the total amount, but also depends largely on the morphological distribution. The environmental effects of different forms are different, which directly affects the toxicity, migration and circulation of heavy metals in the environment (Liu et al. 2016, Xu et al. 2017). The leaching toxicity of Cd in soils before and after remediation showed that the leaching concentration of Cd in the original soils before remediation was much higher than the national standard limit (Table 3) and there was a potential ecological risk. However, the leaching concentration of Cd by TCLP was lower than the limit value of 0.50 mg.kg^{-1} after remediation.

CONCLUSION

The novel remediation agent quickly achieved adsorption equilibrium, had large adsorption capacity, and the specific amino acid functional groups aided in the stabilization of Cd in soil. The TCLP concentration of Cd in the original soil before remediation was far higher than the limit set by the national standard, and there were potential ecological risks. However, the TCLP leaching concentration of Cd in the remediated soil was lower than the international standard. The application of the remediation agent reduced the level of Cd pollution in solid media, reduced the leaching and migration of heavy metals, and achieved the purpose of stabilization remediation.

REFERENCES

Cheng, K., Sun, Z., Zhou, Y., Zhong, H., Kong, X., Xia, P., Guo, Z. and Chen, Q. 2013. Preparation and biological characterization of hollow magnetic Fe$_3$O$_4$@C nanoparticles as drug carriers with high drug loading capability, pH-control drug release and MRI properties. Biomaterials Science, 1(9): 965-974.

Jayasinghe, G.Y., Tokashiki, Y. and Kitou, M. 2009. Evaluation of coal fly ash-based synthetic aggregates as a soil ameliorant for the low productive acidic red soil. Water Air and Soil Pollution, 204 (1-4): 29-41.

Li, W., Tian, Y., Li, P., Zhang, B., Zhang, H., Geng, W. and Zhang, Q. 2015. Synthesis of rattle-type magnetic mesoporous Fe$_3$O$_4$@mSiO$_2$@BiOBr hierarchical photocatalyst and investigation of its photoactivity in the degradation of methylene blue. Rsc. Advances, 5(59): 48050-48059.

Liu, X., Guo, K., Huang, L., Ji, Z., Jiang, H., Li, H. and Zhang, J. 2017. Responses of absolute and specific enzyme activity to consecutive application of composted sewage sludge in a Fluventic Ustochrept. Plos One, 12(5): e0177796.

Liu, W., Wang, S., Lin, P., Sun, H., Hou, J., Zuo, Q. and Huo, R. 2016. Response of CaCl$_2$-extractable heavy metals, polychlorinated biphenyls, and microbial communities to biochar amendment in naturally contaminated soils. Journal of Soils & Sediments, 16(2): 476-485.

Wang, N., Xu, X., Li, H., Wang, Q., Yuan, L. and Yu, H. 2017. High performance and prospective application of xanthate-modified thiourea chitosan sponge-combined, *Pseudomonas putida*, and *Talaromyces amestolkiae*, biomass for Pb(II) removal from wastewater. Bioresource Technology, 233: 58-66.

Xu, Yi, Liang, Xufeng, Xu, Yingying, Qin, Xu, Huang, Qingqing, Wang, Lin and Sun, Yuebing 2017. Remediation of heavy metal-polluted agricultural soils using clay minerals: A review. Pedosphere, 27(2): 193-204.

Yang, T., Shen, C., Li, Z., Zhang, H., Xiao, C., Chen, S., Xu, Z., Shi, D., Li, J. and Gao, H. 2005. Highly ordered self-assembly with large area of Fe$_3$O$_4$ nanoparticles and the magnetic properties. Journal of Physical Chemistry B, 109(109): 23233-23236.

Zhang, J., Zhai, S., Li, S., Xiao, Z., Song, Y., An, Q. and Tian, G. 2013. Pb(II) removal of Fe$_3$O$_4$@SiO$_2$-NH$_2$ core-shell nanomaterials prepared via a controllable sol-gel process. Chemical Engineering Journal, 215-216(1): 461-471.